Tectonophysics, 41 (1977) 79—100

HEAT FLOW AND HEAT PRODUCTION IN ZAMBIA: EVIDENCE FOR LITHOSPHERIC THINNING IN CENTRAL AFRICA

DAVID S. CHAPMAN * and HENRY N. POLLACK

Department of Geology and Mineralogy, The University of Michigan, Ann Arbor, Michigan (U.S.A.)

(Revised version received August 11, 1976)

ABSTRACT

Chapman, D.S. and Pollack, H.N., 1977. Heat flow and heat production in Zambia: evidence for lithospheric thinning in central Africa. In: A.M. Jessop (editor), Heat Flow and Geodynamics. Tectonophysics, 41: 79—100.

Heat-flow results from eleven widely spaced sites in central and western regions of the Republic of Zambia range between 54 and 76 mW m^{-2}. Ten of the sites are located in late Precambrian (Katangan) metasediments or Kibaran age basement, while one site is located in Karroo age sandstone. Compared to the global mean of 39 ± 7 (sd) mW m^{-2} for Precambrian provinces elsewhere, these heat-flow results are anomalously high by some 25 mW m^{-2}. Heat-production measurements on borehole core samples indicate that enhanced radioactivity of an enriched surface zone can account for only half of the observed anomaly. The remaining anomalous heat flow must have a deeper source, and can be interpreted as a flux from the asthenosphere, providing the overlying lithosphere has been thinned to less than 60 km. Such an interpretation supports the existence of an incipient arm of the East African rift system trending southwest from Lake Tanganyika into the central African plateau.

INTRODUCTION

In this paper we describe the results of a program of heat-flow measurements on the central African plateau, undertaken with the dual purpose of extending the heat-flow coverage on the African continent and providing some constraints on geodynamic models of continental rifting. Notwithstanding Bullard's pioneering heat-flow work in South Africa (Bullard, 1939), and subsequent work there and in South West Africa by Carte (1954), Gough (1963), and Carte and Van Rooyen (1971), up until 1967 not a single continental heat-flow result had been published for Africa north of the Limpopo river. Since that time, Beck and Mustonen (1972), Chapman and Pollack (1974), and Sass and Behrendt (in prep.) have conducted measurements

* Present address: Department of Geology and Geophysics, The University of Utah, Salt Lake City, Utah 84112, U.S.A.

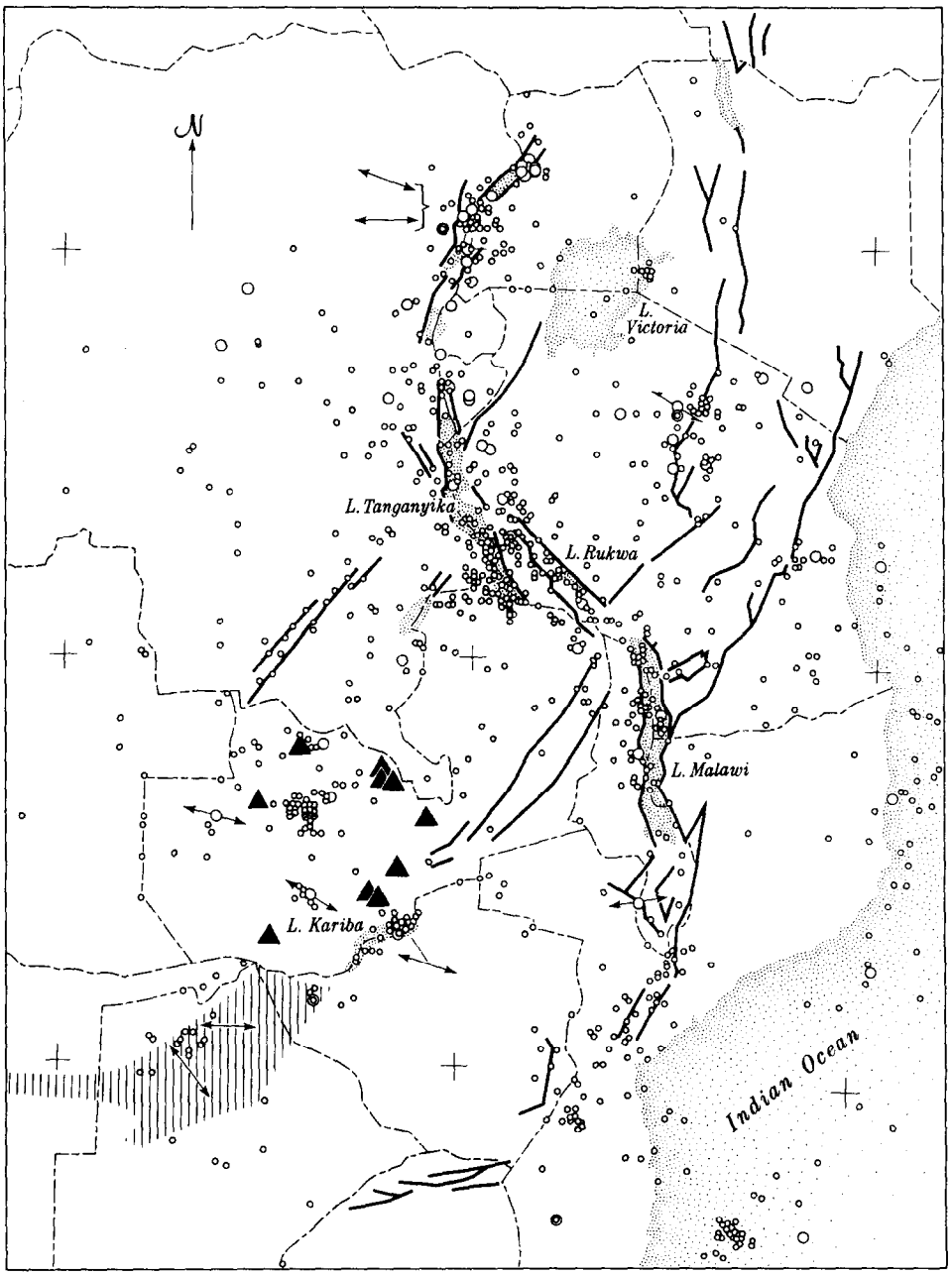

Fig. 1. Tectonics of east and central Africa. Bold lines are faults; small circles ($3 \leqslant m < 5$) and large circles ($5 \leqslant m$) show earthquake epicenters for the period 1965—1970, arrows indicate tensional axis for earthquake-source mechanisms; shaded region is electrical-conductivity anomaly. Triangles locate Zambian heat-flow sites.

in parts of West Africa. In East Africa, Girdler (1970) and Evans and Tammemagi (1974) have reported heat-flow values from the coastal plains of Sudan and Somalia, and Morgan et al. (1973) have conducted heat-flow surveys in and near the Gregory rift in Kenya. Oceanographic techniques have been utilized to make heat-flow measurements in the rift lakes Malawi, Tanganyika, and Kivu (Von Herzen and Vacquier, 1967; Degens et al., 1971, 1973), but unfortunately the large scatter in these data makes interpretation of these results difficult. Prior to the results reported herein, there were no continental heat-flow measurements between the Gregory rift in Kenya and the Republic of South Africa.

This region, from 5° to 25°S and 20° to 35°E, is one of considerable tectonic interest, largely because of the presence of the East African rift system in the eastern part of the region, and because of speculations on a possible southwestward continuation through the region (Fairhead and Girdler, 1969; Scholz et al., 1976). The general location of the region together with some geologic and geophysical indicators of tectonism is shown in Fig. 1. Although the rift system finds topographic expression in a roughly south by southeast line through Lakes Tanganyika, Rukwa, and Malawi, there is a growing body of geophysical evidence that suggests the presence of one or several arms of the rift system extending along southwest trends (cf. Lake Mweru in Zambia and Upemba in Zaire) across the central African plateau, through the Republic of Zambia and northern Botswana. A recently discovered electrical conductivity anomaly (De Beer et al., 1975), and preliminary gravity results from Zambia (I.M. Cowan and H.N. Pollack, personal communication, 1975) both support this tectonic trend. Persuasive evidence for contemporary tectonism can be found in the level of seismic activity and the clear delineation of seismic zones in the central African plateau, which indicate that the region is undergoing substantial tectonic stress release.

To these observations we now add evidence for a broad anomalous heat-flow zone in west and central Zambia, where the heat-flow values are anomalously high by some 50% in comparison to similar age tectonic provinces elsewhere. The anomaly persists after taking the radioactivity of surface rocks into account, and therefore must be due to some deeper source. The interpretation given to this thermal anomaly may be seen to lend support to the hypothesis of incipient rifting in the central African plateau.

TEMPERATURE AND CONDUCTIVITY MEASUREMENTS

Temperature surveys were conducted between 1971 and 1975 in boreholes drilled by mining companies and the Geological Survey of Zambia, usually several weeks to several months after drilling had been completed. Temperatures were measured at 10-m intervals with thermistor probes in combination with a Wheatstone type resistance bridge (for details see Chapman, 1976). The precision of temperature measurements is estimated to

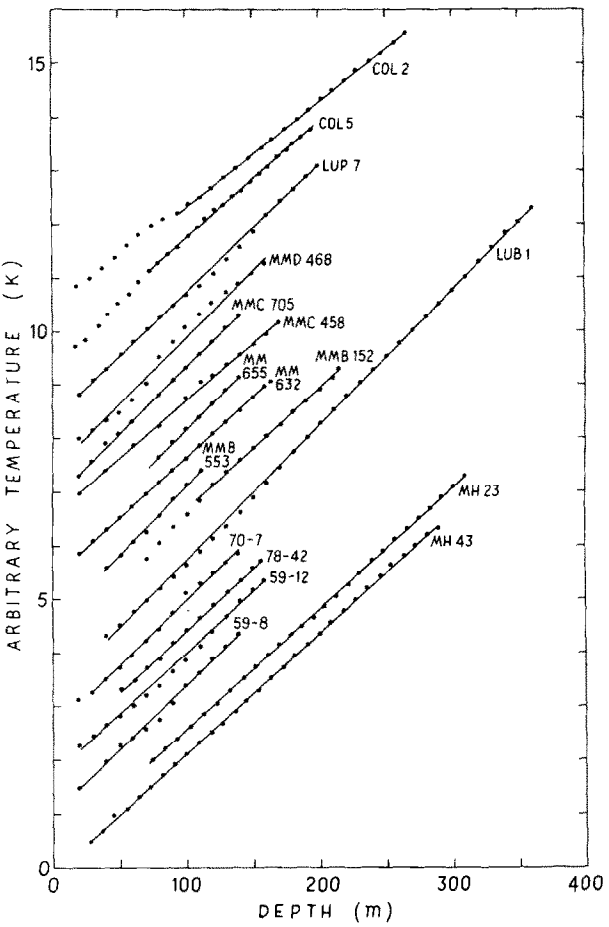

Fig. 2. Temperature–depth curves at selected heat-flow sites. Borehole code and sites include: COL, Mkushi; LUP, Lumpuma; MMD, Lubwe; MMC and MM, Chimiwungo; MMB, Malundwe; LUB, Lubombo; 70-7 etc., Chalalobuka; MH, Munali Hills.

be ±0.01 K whereas the accuracy is probably about ±0.1 K.

Temperature–depth curves for seventeen boreholes at eight sites are shown in Fig. 2. Solid lines have been fitted to the data only for those sections of the borehole ultimately used to calculate heat flow. The geothermal gradients are remarkably uniform among these sites, distributed over a region of several hundred kilometers dimension. All but two of the gradients shown lie within 10% of 22.8 K km^{-1}. The lithologies for most of the boreholes are similar, comprising largely granitic gneisses, biotite gneisses, and mica schists typical of the Precambrian basement complex and lower Katangan system of Zambia (De Swardt and Drysdall, 1964).

The topography at most of the sites is extremely flat, amounting in most

cases to a few tens of meters change in elevation over several kilometers horizontally. The topographic correction (Birch, 1950) to the temperature gradient for borehole MH43, the site with the greatest topographic relief, amounts to only 3%, and therefore such corrections can safely be neglected. No corrections to the temperature gradients for possible climatic change have been applied.

Thermal-conductivity measurements were subsequently made on solid rock discs in a divided bar apparatus similar to that described by Sass et al. (1971). All rocks were saturated with water prior to measurements by allowing water to enter an evacuated vessel containing the samples. Conductivity values were computed relative to the conductivity of fused quartz, for which the Ratcliffe (1959) value was used. Experimental uncertainties for the conductivity measurements are typically 3%.

HEAT-FLOW RESULTS

The heat-flow values were computed as the product of the harmonic mean conductivity (mean resistivity) and the least-squares vertical temperature gradient applied to the entire undisturbed section of the drillhole. The possibility of systematic variation of heat flow with depth was investigated by the interval method in which the above computational procedure was applied sequentially to 30-m intervals of depth throughout the entire borehole. A further consistency check was provided by computing and plotting the thermal resistance integral (Bullard, 1939) for each hole. Both the interval and Bullard methods were of use in discarding upper sections of certain boreholes for which the apparent heat flow either fluctuated widely or departed significantly from the more consistent deeper sections. For the depth ranges finally used in the calculation of heat flow the value reported in this paper agrees with the mean interval heat flow and the resistance integral heat flow to within 5%.

Heat-flow results for 22 boreholes and one mine shaft at eleven distinct sites are presented in Table I. Where several boreholes lie within a 10 km^2 area, a site mean has been calculated, weighted by the reliability of individual borehole values (Beers, 1962, p. 37). The sites Malundwe, Chimiwungo and Lubwe are separated by less than 20 km and for some purposes may be referred to collectively by the regional name Lumwana.

For each borehole the depth range used for calculating heat flow, the number of conductivity samples, the harmonic mean conductivity, and the least-squares temperature gradient is given in Table I in addition to the heat-flow value. The uncertainty associated with an individual heat-flow value in Table I is the standard error of the mean. Twice this uncertainty corresponds to the 95%-confidence level for the mean. At our most reliable sites the scatter between boreholes approaches this value. At other sites, greater scatter in individual heat-flow values indicates the presence of larger uncertainties caused by inadequate sampling or a variety of systematic distur-

TABLE I

Zambia heat-flow data

Locality	Latitude (S)	Longitude (E)	Elevation (m)	Depth range (m)	N	k ($W\,m^{-1}\,K^{-1}$)	$\frac{dT}{dz}$ ($mK\,m^{-1}$)	q ($mW\,m^{-2}$)
Mkushi	13°55′	29°12′	1143 ± 15					mean 61
COL 2				114—279	20	3.24	18.8	61 ± 2
COL 5				64—201	16	2.98	20.5	61 ± 3
Chalalobuka	15°13′	28°33′	1105 ± 15					mean 66
CH 78-42				50—161	11	2.90	22.0	64 ± 7
CH 70-7				30—144	16	3.12	23.0	72 ± 7
CH 59-12				20—164	13	3.11	21.9	68 ± 4
CH 59-8				20—150	7	2.63	23.3	61 ± 6
Lubombo	15°49′	27°55′	1009 ± 3					mean 71
LUB 1				40—360	10	2.81	25.4	71 ± 3
Lumwana *	12°15′	25°51′						mean 57
Malundwe	12°14′	25°49′	1290 ± 10					mean 62
MMB 152				120—208	19	2.65	21.4	57 ± 8
MMB 553				40—113	11	2.76	24.9	69 ± 6
Chimiwungo	12°17′	25°53′	1340 ± 10					mean 55
MM 632				20—163	13	2.43	22.1	54 ± 6
MM 655				60—140	9	2.16	24.0	52 ± 6
MMC 458				20—175	19	2.17	20.5	45 ± 4
MMC 705				20—140	12	2.70	24.7	67 ± 7

Lubwe	12°10′	25°57′	1356 ± 10					mean 54
MMD 468				20—176	18	2.21	24.5	54 ± 6
Lumpuma	13°05′	28°03′	1204 ± 30					mean 65
LUP 7				20—198	19	2.73	23.6	65 ± 4
Munali Hills	15°55′	28°08	1097 ± 15					mean 64
MH 23				70—309	7	2.82	22.6	64 ± 3
MH 43				27—290		2.82 **	22.6	64 ± 3
Ichimpe	12°44′	28°07′	1210 ± 15					mean 74
PE 2				20—500	11	3.89	19.0	74 ± 5
Luanshya Mine	13°05′	28°19′	1256 ± 10					mean 76
28 Shaft ***				0—1150	45	3.30	23.1	76 ± 4
P 38				960—1150	27	3.30	19.8	65 ± 6
BX 168				395—575	7	4.28	17.8	76 ± 5
DH 3465				680—994	15	4.05	20.0	81 ± 5
DH 2231				681—852	20	3.07	18.0	55 ± 8
Machili	16°52′	25°08′	1095 ± 10					mean 67
GS 108				164—302	13	3.00	22.3	67 ± 11

* Lumwana is a regional name for the collection of sites Malundwe, Chimiwungo, and Lubwe.

** Conductivity mean taken from MH 23 samples.

*** Temperatures obtained on seven levels.

Definitions:

N = number of conductivity samples; k = harmonic mean thermal conductivity; dT/dz = least-squares temperature gradient; q = heat flow.

bances (see Sass et al., 1971, for discussion). We estimate the probable uncertainty of most of the site means to be less than 10%, one exception being the Machili value which may be in error by as much as 30%. At Machili the gradient drops steadily from 40 K km^{-1} at 50 m to 22 K km^{-1} at 164 km, although the conductivity shows no appreciable variation with depth. The apparent heat flow is fairly uniform between 164 and 302 m but the disturbance above this interval gives us less confidence in the calculated value.

The heat-flow values for individual boreholes range between 45 and 81 mW m^{-2}, while the site means vary only from 54 to 76 mW m^{-2}. The mean value for the eleven sites is 66 mW m^{-2}. Although this value is not very different from the global mean heat flow of 59 mW m^{-2} (Chapman and Pollack, 1975) it is some 50% higher than heat flow observed in comparable age rocks elsewhere.

TECTONIC SETTING AND THE HEAT-FLOW ANOMALY

Apart from limited areas of Karroo (Permian—Jurassic) sedimentary and volcanic rocks, and Pleistocene Kalahari sands which obscure much of the solid geology in the west, Zambia consists mainly of Precambrian rocks. The country can be divided into five principal structural-stratigraphic provinces (Drysdall et al., 1972): (1) the Bangweulu Block in the north, undisturbed since Ubendian (1800 m.y.) events; (2) The Kibaran province (1300 ± 40 m.y. culmination) comprising a wide variety of granites, gneisses, migmatites, metasediments and metavolcanics making up the pre-Katanga Basement complex in the east and central part of the country; (3) the Katanga system and Lufilian arc lying between the Congo craton to the north and the Kalahari craton to the south, comprising geosynclinal sediments of the Katanga system (1300—620 m.y.) deformed principally during the polyphase Lufilian orogeny which is dated in central Zambia by ages around 720 m.y.; (4) the Mozambique belt (c. 460 m.y.) in the extreme east; and (5) the Karroo basins and troughs which are characteristically fault-bounded asymmetrical downwarps partly filled with sub-horizontal, unmetamorphosed continental sediments and locally overlying basalts. Both the Lufilian arc and the Mozambique belt are considered to be parts of the widespread late Precambrian—early Phanerozoic Pan-African orogeny. For the purpose of subsequent geothermal interpretations we consider the first four of the above provinces together, separate from the post Pan-African terrain. The distribution of all heat-flow sites in relation to this simple tectonic division is shown in Fig. 3. Apart from the site at Machili, which penetrates 300 m of Karroo age sandstones and mudstones, all the other heat-flow stations are situated in Kibaran or Katangan age rocks. Only at the Kibaran Mkushi site has a local isotopic age of 1635 m.y. (Snelling et al., 1964) been determined. The Katangan heat-flow sites probably represent an age spread from 730 ± 50 m.y. in the south to 520 ± 50 m.y. in the north based on geologic correlation

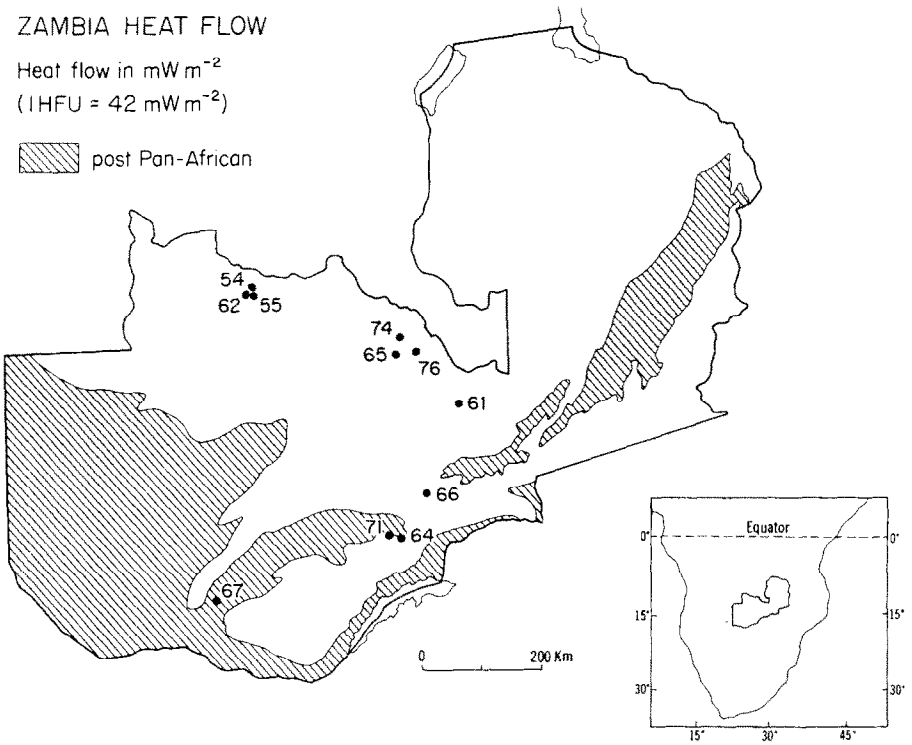

Fig. 3. Location map of the Republic of Zambia showing heat-flow sites, heat flow values in mW m^{-2}, Precambrian (unshaded) and post Pan-African (shaded) terrains.

with other areas which have been radiometrically dated.

The tectono-thermal history of heat-flow sites is important because it provides the basis for one of the most important continental heat-flow correlations: that of decreasing heat flow from tectonic elements of increasing age. The most detailed exposition of this relationship is that of Polyak and Smirnov (1968), who divided continental heat-flow values into subsets corresponding to the age of most recent mobilization. They found the values to be normally distributed about the means of the subset, and the subset means to show a systematic decrease with increasing age (Fig. 4). This general relationship has several difficulties when the data are analyzed in detail: the age trend does not seem to apply within individual subsets such as Precambrian shields (Rao and Jessop, 1975); and although the subset values are distributed normally in a statistical sense, the low heat-flow values in a subset may have tectonic significance quite separate from the high values, as for example in the Sierra Nevada Mountains of the western U.S.A. (Blackwell, 1971). In spite of these difficulties the overall trend seems to be genuine, and we utilize it in the following section.

In Fig. 4 we plot the mean value of 66 mW m^{-2} for our ten Precambrian

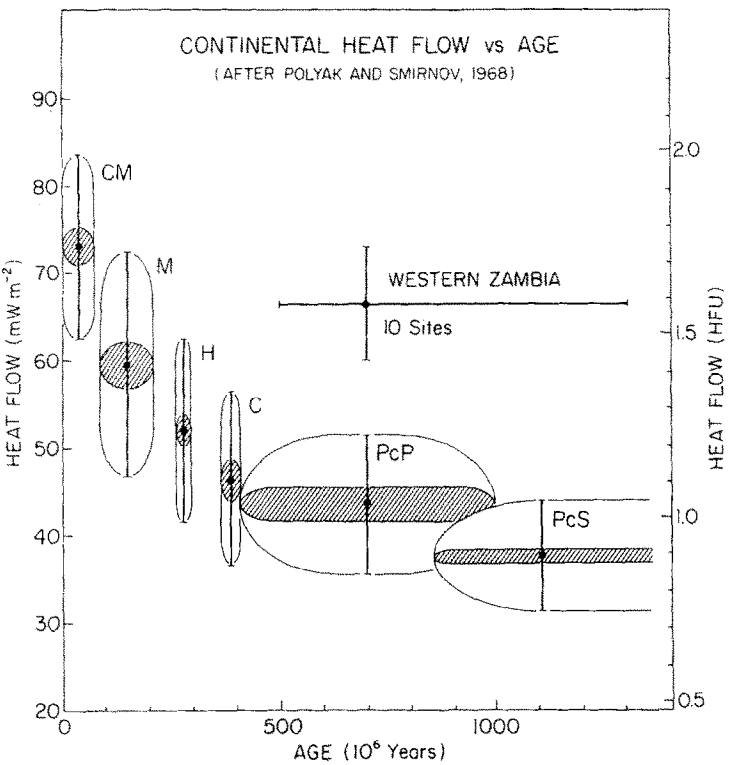

Fig. 4. Mean heat flow from the ten Zambian Precambrian sites superimposed on plot of heat flow against age of tectonogenesis after Polyak and Smirnov (1968). Tectonic provinces include: PcS, Precambrian shield; PcP, Precambrian platform; C, Caledonian folding; H, Hercynian folding; M, Mesozoic folding; CM, Cenozoic miogeosyncline. Shaded ellipse represents standard error of the mean heat flow; vertical bar and open ellipse represents standard deviation.

sites at a collective representative age of 700 m.y. The standard deviation of the individual heat-flow values and standard error of the mean are 7 and 2.3 mW m^{-2} respectively. It is apparent from Fig. 4 that the Zambian surface heat flow is anomalously high, exceeding the mean heat flow for Precambrian shields and platforms by 27 and 22 mW m^{-2} respectively.

Before attaching a tectonic significance to this high heat flow we must estimate what fraction of the anomaly, if any, is caused by enhanced heat production in the near-surface rocks. We therefore turn now to the results of our heat-production measurements.

HEAT PRODUCTION

The radioactive heat generation of representative rocks from the heat-flow sites was determined by gamma-ray spectroscopy methods. Measurements

were normally made on 1 kg aggregate crushed samples comprising several individual specimens collected at regular intervals along the drill core. Measurement uncertainties were reduced to 2% by employing appropriately long counting times. Uncertainty due to sampling bias is more difficult to estimate, but we believe it is limited to about 15% by the use of the composite sample. Detailed results of fourteen heat-production determinations from the heat-flow sites are given in Table II. For each determination the site or drillhole, the number of samples in the composite predominant rock type, the U, Th, and K concentrations and computed heat generation is given. Heat-production values were calculated from the measured abundances of uranium, thorium, and potassium using the relation (after Birch, 1954):

$$A = 0.01\,\rho(9.69\mathrm{U} + 2.65\mathrm{Th} + 3.58\mathrm{K})$$

where A is heat production in μW m^{-3}, ρ is density in g cm^{-3}, U is uranium concentration in ppm, Th is thorium concentration in ppm, and K is potassium content in percent.

The majority of the samples consist of granite gneisses, biotite gneisses, mica schists and amphibolites belonging to the pre-Katanga basement and Katanga metasediments. In some cases the aggregate samples from the borehole drill core typify the regional geology of the site for several kilometers around and are used directly for the site mean value. In other cases the boreholes penetrate rock that is very localized in vertical and horizontal extent, and in such cases the site mean is weighted by the regional extent of certain rock types. We realize the subjective approach to such a weighting procedure and have therefore attempted to overestimate heat production, which will have the effect of minimizing our reduced heat-flow anomaly. The affected sites are Lumpuma, where the low value for the localized gabbro in which the borehole was situated has been neglected in computing the site mean, and Munali Hills where the boreholes penetrate a gabbro sill which is also thought to be of limited extent. In the latter site, the value of 2.4 μW m^{-3} for the biotite schist composite sample at Lubombo 15 km away, which coincides with the mean value for basement rocks elsewhere, is considered to be a more representative value.

It is now appropriate to judge how much, if any, of the apparent surface heat-flow anomaly of about 25 mW m^{-2} (Fig. 4) arises from the near-surface radiogenic sources and how much has a deeper origin. It is well known that large variations in surface heat flow can arise merely from differences in heat production of a near-surface enriched zone. Furthermore, in order to distinguish genuine differences between various continental regions, it is desirable to determine the parameters q^* and b (the reduced heat flow and characteristic depth of the heat-source distribution, respectively) of the empirically determined linear heat-flow—heat-production relation:

$$q_0 = q^* + bA_0$$

where q_0 is the surface heat flow and A_0 the surface heat production.

TABLE II

Zambia heat-production data

Site	*N*	Depth range (m)	Rock type	U (ppm)	Th (ppm)	K (%)	*A* ($\mu W\ m^{-3}$)
Mkushi							mean 1.9
COL 2	25	52—310	granitic and biotitic gneiss	4.1	6.2	3.3	1.8
COL 5a	15	23—145	granitic and biotitic gneiss	3.7	9.0	2.9	1.9
COL 5b	11	158—270	granitic and biotitic gneiss	3.7	8.8	3.3	1.9
Chalalobuka							mean 2.3
CHAL 1 *	22	41—165	biotite and amphibolite schists, granite gneiss	5.4	8.7	2.7	2.3
Lubombo							mean 3.6
LUB 1a	1	248	granite	6.8	13.2	4.7	3.2
LUB 1b	10	43—185	biotite schist	3.4	17.4	3.4	2.4
LUB 1c	13	205—382	granite, amphibolite	7.7	40.3	4.0	5.2
Lumwana							mean 2.5
LUMW 1 **	10	31—162	mica schists	4.5	13.2	3.7	2.5
Lumpuma							mean 1.8 ***
LUP 7a	7	30—134	garnet mica schists	1.6	15.3	2.7	1.8
LUP 7b	8	15—195	gabbro	1.4	7.6	1.9	1.1
Munali Hills							mean 2.4 ***
MH 23a	10	18—108	quartzite, schists	1.5	5.7	1.5	0.94
MH 23b	13	124—324	gabbro	0.3	0.9	0.3	0.16
MH 43a	8	45—162	gabbro	0.3	0.8	0.3	0.16
MH 43b	8	178—296	gabbro	0.6	1.6	0.3	0.29

* Samples from boreholes CH 70-7, CH 59-12, CH 59-8.

** Samples from boreholes MMB 152, MMB 553, MMD 468, MMC 705, MMC 458.

*** See text for discussion.

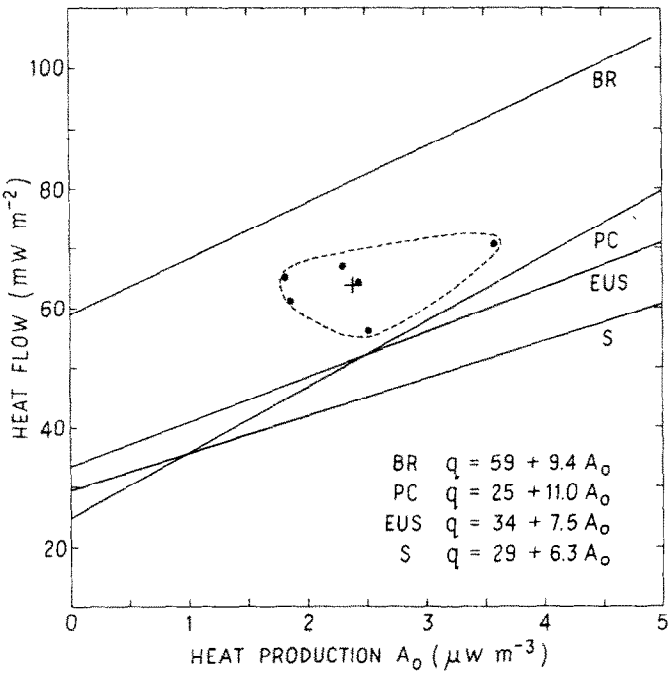

Fig. 5. Heat flow and heat-production results showing individual site values (●) and the mean value (+) for six Zambian sites. Lines representing linear heat-flow relationships include: BR, Basin and Range; PC, all published Precambrian sites; EUS, Eastern United States; S, all shields.

In Fig. 5 we have plotted heat flow versus representative heat production for the six sites where information is available. The clustering of heat-flow values in our study precludes a meaningful estimation of q^* and b by fitting a straight line to our data points. Instead, the non-radiogenic part of the Zambian heat-flow anomaly must be inferred by comparison with results obtained elsewhere. We explore two types of comparison: the first is a direct comparison of the Zambian heat-flow—heat-production results with heat-flow—heat-production trends in other continental regions; the second is a comparison with typical heat-production values alone.

The first comparison may be seen directly in Fig. 5. Three previously published lines representing heat-flow—heat-production relationships have been included: Basin and Range, $q_0 = 59 + 9.4A_0$ (Roy et al., 1968); eastern U.S.A., $q_0 = 34 + 7.5A_0$ (Roy et al., 1968); and all shields, $q_0 = 29 + 6.3A_0$ (Rao and Jessop, 1975). In these equations, q_0, q^*, b and A_0 have units of mW m^{-2}, mW m^{-2}, km, and μW m^{-3}, respectively. A fourth line $q_0 = 25 + 11A_0$ is included which is a line fit to all published Precambrian heat-flow—heat-production pairs (Jessop et al., 1976) exclusive of Zambia. The parameters of this line are strongly influenced on the low heat-production end by

results from southern Norway (Swanberg et al., 1974) and Niger (Chapman and Pollack, 1974) and on the high end by the highly radioactive sites in central Australia (Jaeger, 1970). All the individual Zambian results lie systematically above the curves for the old stable regions, and the departure of the mean heat flow from these lines is between 13 and 20 mW m^{-2} depending on which line is chosen as a reference. This departure is thus an estimate of the residual anomaly not attributable to enhanced near-surface radioactivity.

The alternative method compares the average abundance of U, Th, and K in large surface areas of old continental regions with the mean heat production value of 2.4 μW m^{-3} for the Zambian sites. Such a method may avoid biasing from the very restricted heat-flow—heat-production site distribution on shields. Shaw (1967) has estimated 1.6 μW m^{-3} as a mean heat production for the surficial exposure of the Canadian shield, while Heier and Rogers (1963) obtained 1.7 μW m^{-3} as a mean for all continental regions. Thus the Zambian terrain appears to have a surface heat-production enhancement ΔA_0 of 0.7—0.8 μW m^{-3}. The enhanced fraction of the radioactive surface layer in the steady state contributes $b\Delta A_0$ to the surface heat flux independent of the actual vertical distribution, whether it be a stepwise, linear, or exponential decrease with depth. Using values of $\Delta A_0 = 0.8$ μW m^{-3} and $b =$ 11 km, this enhancement can account for only 9 mW m^{-2} of the original 22—27 mW m^{-2} surface heat-flow anomaly, leaving a residual anomaly of 13—18 mW m^{-2}.

Thus, from both of the above comparisons we deduce that enhanced heat production from the surface layer can account for less than half of the Zambian surface heat-flow anomaly, and that a residual heat-flow anomaly of 15 mW m^{-2} or greater persists. It is even less likely that the anomaly arises from unusual radioactivity at greater depths. The lower crust is thought to consist of granulite facies rocks (see Smithson and Decker, 1974, for discussion) with characteristic heat-production values between 0.2 and 0.5 μW m^{-3}. As this represents a radiogenic depletion by a factor of 5—10 relative to upper crustal rocks it is unlikely that the source of the residual heat flow is radiogenic in the crust. The same argument holds true for the upper mantle which is likely to be depleted by another factor of 10 below the lower crust concentrations. We therefore believe that the source of the anomaly is tectonic rather than radiogenic, and that the probable source of the anomaly is a zone of elevated temperatures at depth resulting from an intrusion from or some thermal process in the asthenosphere.

TEMPERATURE-PERTURBATION MODELS

We consider two interpretive models involving temperature perturbations at depth to explain the broad observed heat-flow anomaly. In the plate-tectonic framework our first model corresponds to the lithosphere coming to rest over an asthenospheric hotspot or convective upwelling. Burke and

Wilson (1972) suggest that such an event happened to the African plate 25 m.y. ago. In support of their hypothesis they cite such geologic evidence as the termination of the Walvis ridge just east of magnetic anomaly 6, the lack of Neogene volcanic traces within the African plate, the changed pattern of Indian Ocean spreading, and the marked increase in volcanic activity, all occurring about 25 m.y. ago.

The first model involves the computation of surface heat flow in time following a sudden increase in temperature at the base of a slab. The transient response of the surface gradient is given (after Carslaw and Jaeger, 1959, p. 99) by:

$$\left.\frac{\partial T}{\partial z}\right|_{z=0} = \frac{\Delta T}{l}\left[1 + 2\sum_{n=1}^{\infty}(-1)^n \exp\left(-n^2\pi^2\frac{\alpha t}{l^2}\right)\right]$$

where ΔT is the temperature step at $z = l$, l is the slab thickness, α thermal diffusivity, and t is time elapsed since the temperature step occurred. This solution is shown in Fig. 6 for $\Delta T = 100$ K and $\alpha = 32$ km^2/m.y.; the time t (m.y.) identifies individual curves. The equilibrium surface gradient perturbation ($t = \infty$) is inversely proportional to the slab thickness, and as the slab thickness increases a progressively longer time is required before the full effect is seen at the surface.

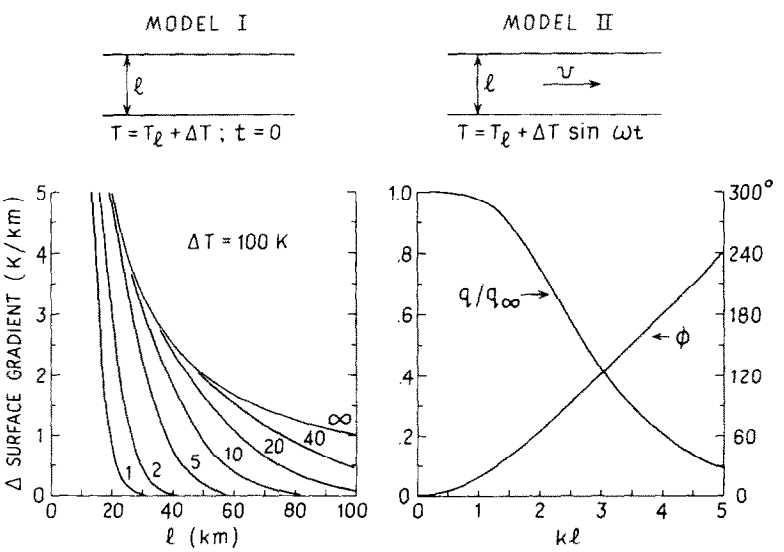

Fig. 6. Thermal models showing response at the surface to specified temperature perturbations at depth. Model I: Step temperature perturbation at base of slab l km thick. Curves are labeled by time (m.y.) since start of perturbation, and give change in surface gradient. Model II: Time periodic perturbation at base of slab l km thick. Curves give attenuation q/q_∞ and phase shift ϕ of the surface heat flow as functions of a dimensionless parameter kl (defined in text).

To explain the Zambian anomaly of 15 mW m^{-2}, assuming a mean thermal conductivity of 3 W m^{-1} K^{-1}, we seek conditions capable of producing a surface gradient perturbation of 5 K km^{-1}. Although the set of conditions is not unique, we can find a limiting depth below which the temperature perturbation required to produce the observed surface anomaly becomes unacceptably large. For example, if 300 K represents a reasonable upper limit to the size of the temperature step then the steady surface gradient perturbation of 1.67 K km^{-1}/100 K step (i.e. 5 K km^{-1}/300 K step) in Fig. 5 limits the source to depths less than 60 km. Correspondingly shallower depths to the temperature perturbation are required if the anomaly is still in a transient state: e.g. the depth must be 50 km for a step 20 m.y. ago, and 33 km for a step 5 m.y. ago.

Our second model involves a temperature perturbation that is spatially periodic at the base of a moving slab (Pollack and Chapman, 1974). This corresponds to the lithosphere moving over a regular spatially periodic array of hotspots and coldspots in the asthenosphere, which a given element of lithosphere sees as an oscillatory (time periodic) lower boundary condition. This results in an upward propagating thermal wave which is both attenuated and phase-shifted at the surface. The temperature perturbation T is given (after Carslaw and Jaeger, 1959, p. 105) by:

$$T = A(z) \sin[\omega t - \phi(z)]$$

where:

$$\begin{matrix} A(z) \\ \phi(z) \end{matrix} = \begin{matrix} \mathrm{mod} \\ \arg \end{matrix} \left[\frac{\sinh kz\,(1+i)}{\sinh kl\,(1+i)}\right]$$

and:

$$k = \left(\frac{\omega}{2\alpha}\right)^{1/2} = \left(\frac{\pi}{\alpha\tau}\right)^{1/2}$$

The thermal-wave number k depends on the thermal diffusivity α and the period τ, which may be thought of as the time taken for an element of lithosphere to pass from hotspot to hotspot. The perturbed temperature gradient at the surface due to the periodic disturbance at depth is not conveniently expressed, but is easily computed. Figure 6 shows the ratio of surface flux q to the equilibrium flux q_∞ of an infinitely long period wave (i.e.: a steady perturbation) and the surface phase shift as functions of the dimensionless parameter kl. The value of kl depends explicitly on the slab thickness l, and the period of the disturbance, which in turn is dependent on the spacing between hot spots and the velocity of the plate. The values of kl that obtain for a hotspot spacing of 1000 km and for a range of slab thickness and relative velocities are given in Table III.

Allowing for uncertainty in the spatial characteristics of the source array, it appears that the geophysically interesting values of kl lie between 0 and perhaps 20. It is apparent from Fig. 6, however, that observable heat-flow

TABLE III

Values of the dimensionless parameter kl for gephysically relevant combinations of plate thickness and plate velocities

Plate thickness	Plate velocity relative to source		
	fast (10 cm/yr)	slow (1 cm/yr)	very slow (0.1 cm/yr)
50 km	5	1.6	0.5
100 km	10	3.2	1.0
150 km	15	4.8	1.5

anomalies will be associated only with parameters less than about 3, as rapid thermal disturbances at the base of the lithosphere are unlikely to be seen as heat-flow perturbations at the surface, due to the attenuation of the upward propagating thermal wave. With respect to the Zambian anomaly, the effect of this attenuation would be to place a restriction on the depth to the spatially periodic perturbation and on the velocity at which the plate moves across it. The parameter kl can be no greater than 1 if the disturbance is at 60 km depth, and the observed surface heat-flow anomaly is to be accounted for. For l = 60 km, the wavenumber constrains the basal perturbation to a period greater than 350 m.y., or equivalently to a plate velocity less than 0.3 cm yr^{-1} over a hotspot array with characteristic spacing of 1000 km. If kl is assumed to have a value greater than about 3, corresponding to plate motions of a few centimeters a year relative to the source array, then the increased attenuation of the thermal wave requires considerably shallower source depths to obtain the necessary surface heat-flow anomaly. For still greater value of kl no appreciable heat-flow anomaly will appear at the surface. Whichever of the two models we have examined is applicable, the corresponding source of the thermal anomaly cannot lie deeper than about 60 km, and if the source is an intrusion from or the upper boundary of the asthenosphere, it represents a considerable penetration into, or thinning of a Precambrian age continental lithosphere.

AFRICAN RIFT SYSTEM

High heat flow in Zambia resulting from a lithospheric thinning and/or penetration is consistent with other indications mentioned briefly in the introduction that the central African plateau south of Lake Tanganyika is in a dynamic state and responding to contemporary stress. In Fig. 1 we have compiled geophysical data which places the central African plateau in context with the entire African rift system south of the equator.

The seismic activity of the system is represented by the epicenters of earthquakes of magnitude 3.0 or greater for the period 1965 to 1970 as listed in the International Seismological Centre (Edinburgh) Regional

Catalogue of Earthquakes. Notwithstanding the general diffuse nature of the seismicity the epicenters fall into recognizable zones with aseismic regions marking the more stable areas of the Kaapvaal, Rhodesia, Tanzania and Congo cratons. One distinct seismic belt follows the topographic Western Rift and leads southward into Mozambique. A second zone of earthquake activity extends south and west of the above-mentioned belt in three roughly parallel southwest trending bands: along the Upemba trough in southeastern Zaire; from Lake Tanganyika through Lake Mweru with a pronounced concentration in western Zambia; and along the Luangwa valley, through the Middle Zambezi valley and into northern Botswana.

Earthquake-source mechanisms are available for eight large earthquakes in the area shown in Fig. 6, including four from western and southern Zambia (Maasha and Molnar, 1972, table 1). These mechanisms imply a predominantly WNW—ESE tensional pattern accompanied by normal faulting. A recent microearthquake study by Scholz et al. (1975) in Botswana has provided two additional composite source mechanisms from microearthquakes in northeastern Botswana which are consistent with the pattern to the north. This latter study also determined that microearthquake activity as far south as Lake Ngami is presently at a comparable level to that in the East African section of the rift. It appears therefore that the rift system seismicity extends to about 23°S and is roughly constant in level and source mechanisms throughout.

Two studies are available on the propagation of seismic waves throughout the rift system. Gumper and Pomeroy (1970) found East Africa to be characterized by low P_n velocities, poor S_n propagation north of the equator, and comparatively high S_n attenuation in non-rift zones. Examination of their results (Gumper and Pomeroy, 1970, fig. 10) does not reveal direct correlation between regions of poor S_n propagation and the geographical extent of the surficial rift features. Also, Zambia seems to be a mixed region with some paths showing good S_n propagation and others poor. A similar pattern of seismic velocities was obtained by Fairhead and Girdler (1971) using travel-time delays for paths with epicentral distance less than 30°. They mapped regions of low P_n and found especially pronounced low velocities in the Gregory Rift north of 5°S, but found no anomalous propagation in the region between the Eastern and Western rifts, nor to the south of the volcanic zones in Kenya.

A recent magnetometer array study (De Beer et al., 1975) has revealed an electrical conductivity anomaly at crustal depths crossing from South West Africa into Botswana and western Rhodesia. The extent of this anomalous conductor is also shown in Fig. 1. From west to east the conductive zone has an east—west arm running through South West Africa which broadens south of the Okavango delta and turns northward, roughly in line with the northeast—southwest Luangwa—Middle Zambezi rift lineament. However, this northeast trending conductivity anomaly is broader by a factor of 2—3 than the surficial rift features, and is in equally good alignment with several of the

anomalous heat-flow sites. The origin of a conductivity anomaly may be either thermal or compositional or both, the former being associated with anomalously high temperatures in the crust and upper mantle, and the latter with conductive materials which are often concentrated in fracture zones. The actual determination of origin thus often depends on auxillary geophysical and geological evidence. For example, conductivity anomalies under the Kenya Rift (Banks and Ottey, 1974) are interpreted as zones of partial melting in the upper mantle because they coincide with the low-velocity and low-density zones indicated by seismic and gravity investigations and are closely related spatially to regions of late Quaternary volcanic activity. De Beer et al. (1975) prefer a fracture zone for the Botswana anomaly, but our new heat-flow data suggest that the origin may be at least partly thermal. A magnetometer array study across Zambia could provide the necessary complementary data to determine whether the Botswana conductivity anomaly is confined to the Zambezi—Luangwa trend, or whether it broadens to the northwest across the heat-flow anomaly.

Not shown on Fig. 6, but important to a discussion of rifting, are the results of gravity investigations. The recently completed reconnaissance gravity survey of Zambia forms an important link between the extensive work in East Africa (see Wohlenberg, 1975, for summary) and the national surveys of Malawi (Andrews, 1974) and Botswana (Reeves and Hutchins, 1975). Although interpretation of the Zambian data is still in progress, some salient observations can be made. We observe significant differences within Zambia between Bouguer anomaly vs. elevation regressions in rift (Luangwa, Zambezi) and non-rift settings. These regression differences are similar in nature to those described for Kenya by Khan and Mansfield (1971) who have used the differences to infer abnormal crustal structure within the Gregory Rift. Two other features pertinent to rifting hypotheses are the existence of a strong gravity low in a topographically flat region to the south of the western Zambia epicenter cluster, probably indicating a buried NE trending Karroo age trough, and the distinct gravimetric break corresponding to the known surface geologic interruption between the lower Luangwa and middle Zambezi valley, indicating an en-echelon configuration similar to the Rukwa and Tanganyika rifts, rather than a continuity of structure.

SUMMARY AND SPECULATIONS

Several hypotheses have been advanced concerning the southern termination of the East African rift system. A popular plate construction (Dietz and Holden, 1970) pictures the African Rift running through Lake Malawi and the Shire Rift to the Mozambique channel, thereby delineating the southwest boundary of the Somalia subplate. An alternative suggestion is that an arm of the active rift extends southwestward from Lake Tanganyika across the central African plateau (Fairhead and Girdler, 1969). A variant of this alternative suggestion is that the Luangwa—Middle Zambezi lineament marks

a propagating rift extension through eastern and southern Zambia into Botswana (Scholz et al., 1976). Yet another alternative which has received recent attention (Girdler, 1975) is that the long-wavelength negative Bouguer gravity anomaly that is so prominent on the African gravity map of Sletene et al. (1973) may indicate the presence of an incipient rift to the west-southwest of Lake Tanganyika. Over East Africa this negative gravity anomaly coincides with surface rift features and has been interpreted as indicating regions of thinned lithosphere.

There is some, although not equivalent, support for each of the suggested trends. The southern trend through Malawi and Mozambique is supported by strong seismicity, and Quaternary surface rift features. The southwest trend through Zambia and into Botswana is supported by the alignment of the Botswana electrical-conductivity anomaly, long-wavelength residual gravity trends in Zambia, and by seismicity of the area, much of which is unrelated to present fault zones. The western trend is supported only by the topography and the large negative Bouguer gravity anomaly.

Our discovery of a broad heat-flow anomaly and our inference of the thinned lithosphere in west and central Zambia, provides additional support for the southwest rift extension hypothesis. The extent of the thermal anomaly is presently unbounded in all directions except to the southeast where current work (E.R. Oxburgh, personal communication, 1975) indicates normal to sub-normal heat flow on the Rhodesian craton. An important objective for future heat-flow and other geophysical measurements in central Africa will be to prove the extent of the anomalous thermal zone and to discriminate between the rift extension hypotheses.

ACKNOWLEDGMENTS

This project was initiated while we were at the University of Zambia. The fieldwork could not have been completed without the excellent cooperation of our colleagues, and numerous geologists in the Geological Survey of Zambia, Nchanga Consolidated Copper Mines, Roan Consolidated Mines, and Mkushi Copper Mines. In particular, we thank Professor A.H. Ward of the University of Zambia for his support and encouragement throughout the project. Professor R.F. Roy made the radiogenic heat-production measurements. Financial support was provided by the universities of Zambia and Michigan, and the US National Science Foundation, Earth Science Section, under Grant GA-36360.

REFERENCES

Andrews, E.M., 1974. Gravity survey of Malawi: fieldwork and processing. Inst. Geol. Sci. London, Rep., 74/15.

Banks, R.J. and Ottey, P., 1974. Geomagnetic deep sounding in and around the Kenya rift valley. Geophys. J., 36: 321–335.

Beck, A.E. and Mustonen, E., 1972. Preliminary heat flow from Ghana. Nature Phys. Sci., 235: 172–174.

Beers, Y., 1962. Introduction to the Theory of Error. Addison-Wesley, Reading, Mass.

Birch, F., 1950. Flow of heat in the Front Range, Colorado. Geol. Soc. Am. Bull., 61: 567–630.

Birch, F., 1954. Heat from radioactivity. In: H.F. Faul (editor), Nuclear Geology. Wiley, New York, p. 148.

Blackwell, D.D., 1971. The thermal structure of the continental crust. In: J.G. Heacock (editor), The structure and Physical Properties of the Earth's Crust. Geophys. Monogr. 14. American Geophysical Union, Washington, pp. 169–184.

Bullard, E.C., 1939. Heat flow in South Africa. Proc. R. Soc. London, Ser. A, 173: 474–502.

Burke, K. and Wilson, J.T., 1972. Is the African plate stationary? Nature, 239: 387.

Carslaw, H.S. and Jaeger, J.C., 1959. Conduction of Heat in Solids. Oxford University Press, Oxford, 2nd ed., 510 pp.

Carte, A.E., 1954. Heat flow in the Transvaal and Orange Free State. Proc. Phys. Soc. B. 67: 664–672.

Carte, A.E. and Van Rooyen, A.I.M., 1971. Further measurements of heat flow in South Africa. J. Mine Ventilation Soc. South Africa, July: 94–98.

Chapman, D.S., 1976. Heat Flow and Heat Production in Zambia. Ph.D. thesis, University of Michigan.

Chapman, D.S. and Pollack, H.N., 1974. Cold spot in West Africa: anchoring the African plate. Nature, 250: 477–478.

Chapman, D.S. and Pollack, H.N., 1975. Global heat flow: a new look. Earth Planet. Sci. Lett., 28: 23–32.

De Beer, J.H., Gough, D.I. and Van Zijl, J.S.V., 1975. An electrical conductivity anomaly and rifting in southern Africa. Nature, 255: 678–680.

Degens, E.T., Von Herzen, R.P. and Wong, H.K., 1971. Lake Tanganyika: water chemistry, sediments, geologic structure. Naturwissenschaften, 58: 229–240.

Degens, E.T., Von Herzen, R.P., Wong, H.K., Deuser, W.G. and Jannasch, H.W., 1973. Lake Kivu: structure, chemistry and biology of an East African rift lake. Geol. Rundsch., 62: 245–277.

De Swardt, A.M.J. and Drysdall, A.R., 1964. Precambrian geology and structure in central northern Rhodesia. Geol. Surv. Northern Rhodesia Mem., 2: 82 p.

Dietz, R.S. and Holden, J.C., 1970. The breakup of Pangea. Sci. Am., 223: 30–41.

Drysdall, A.R., Johnson, R.L., Moore, T.A. and Thieme, J.G., 1972. Outline of the geology of Zambia. Geol. Mijnbouw, 51: 265–276.

Evans, T.R. and Tammemagi, H.Y., 1974. Heat flow and heat production in northeast Africa. Earth Planet. Sci. Lett., 23: 349–356.

Fairhead, J.D. and Girdler, R.W., 1969. How far does the Rift System extend through Africa? Nature, 221: 1018–1020.

Fairhead, J.D. and Girdler, R.W., 1971. The seismicity of Africa. Geophys. J., 24: 271–301.

Girdler, R.W., 1970. A review of Red Sea heat flow. Philos. Trans. R. Soc. Lond., Ser. A, 267: 191–203.

Girdler, R.W., 1975. The great negative Bouguer gravity anomaly over Africa. Trans. Am. Geophys. Union, 56: 516–519.

Gough, D.I., 1963. Heat flow in the southern Karroo. Proc. R. Soc. Lond., Ser. A, 272: 207–230.

Gumper, F. and Pomeroy, P.W., 1970. Seismic wave velocities and earth structure on the African continent. Bull. Seismol. Soc. Am., 60: 651–668.

Heier, K.S. and Rogers, J.W., 1963. Radiometric determination of thorium, uranium and potassium in basalts. Geochim. Cosmochim. Acta, 27: 137–154.

Jaeger, J.C., 1970. Heat flow and radioactivity in Australia. Earth Planet. Sci. Lett., 8: 285—292.

Jessop, A.M. Hobart, M.A. and Sclater, J.G., 1976. The world heat-flow data collection — 1975. Geothermal Series Number 5, Ottawa, Canada, 125 pp.

Khan, M.A. and Mansfield, J., 1971. Gravity measurements in the Gregory rift. Nature Phys. Sci., 229: 72—75.

Maasha, N. and Molnar, P., 1972. Earthquake fault parameters and tectonics in Africa. J. Geophys. Res., 77: 5731—5743.

Morgan, P., Williamson, K.H., Evans, T.R. and Wheildon, J., 1973. Preliminary heat-flow studies in and around the Kenya rift. Abstr. 1st Meet. Europ. Geophys. Soc., Zurich, p. 71.

Pollack, H.N. and Chapman, D.S., 1974. To what extent does the lithosphere mask lateral variations of temperature in the asthenosphere? Trans. Am. Geophys. Union, 55: 1193.

Polyak, B.G. and Smirnov, Ya.B., 1968. Relationship between terrestrial heat flow and the tectonics of continents. Geotectonics, 4: 205—213.

Rao, R.U.M. and Jessop, A.M., 1975. A comparison of the thermal character of shields. Can. J. Earth Sci., 12: 347—360.

Ratcliffe, E.H., 1959. Thermal conductivities of fused and crystalline quartz. Br. J. Appl. Phys., 10: 22—25.

Reeves, C.V. and Hutchins, D.G., 1975. Crustal structures in central southern Africa. Nature, 254: 408—410.

Roy, R.F., Blackwell, D.D. and Birch, F., 1968. Heat generation of plutonic rocks and continental heat flow provinces. Earth Planet. Sci. Lett., 5: 1—12.

Sass, J.H. and Behrendt, J.C., in preparation. Geothermal data from the Liberian Precambrian shield.

Sass, J.H., Lachenbruch, A.H., Munroe, R.J., Greene, G.W. and Moses, T.H. Jr., 1971. Heat flow in the Western United States. J. Geophys. Res., 76: 6376—6413.

Scholz, C.H., Koczynski, T.A. and Hutchins, D.G., 1976. Evidence for incipient rifting in southern Africa. Geophys. J., 44: 135—144.

Shaw, D.M., 1967. U, Th, and K in the Canadian Precambrian shield and possible mantle compositions. Geochim. Cosmochim. Acta, 31, 1111.

Sletene, R.L., Wilcox, L.E., Blouse, R.S. and Sanders, J.R., 1973. Bouguer gravity anomaly map of Africa. Tech. Paper 73-3, U.S. Defense Mapping Agency.

Smithson, S.B. and Decker, E.R., 1974. A continental crustal model and its geothermal implications. Earth Planet. Sci. Lett., 22: 215—225.

Snelling, N.J., Hamilton, E.I., Drysdall, A.R. and Stillman, C.J., 1964. A review of age determinations from Northern Rhodesia. Econ. Geol., 59: 961—981.

Swanberg, C.A., Chessman, M.D., Simmons, G., Smithson, S.B., Gronlie, G. and Heier, K.S., 1974. Heat flow—heat generation studies in Norway. Tectonophysics, 23: 31—48.

Von Herzen, R.P. and Vacquier, V., 1967. Terrestrial heat flow in Lake Malawi, Africa. J. Geophys. Res., 72: 4221—4226.

Wohlenberg, J., 1975. Geophysikalische Aspekte der ostafrikanischen Grabenzonen. Geol. Jahrb. E, 4: 82 pp.